Universality and hysteresis in slow sweeping of bifurcations

Roie Ezraty,[1] Ido Levin,[1,2] and Omri Gat[1]
[1]*Racah Institute of Physics, Hebrew University of Jerusalem, Jerusalem 9190401, Israel*
[2]*Department of Chemistry, University of Washington, Seattle, Washington 98195, USA*

(Received 1 September 2023; accepted 21 March 2024; published 9 April 2024)

Bifurcations in dynamical systems are often studied experimentally and numerically using a slow parameter sweep. Focusing on the cases of period-doubling and pitchfork bifurcations in maps, we show that the adiabatic approximation always breaks down sufficiently close to the bifurcation, so the upsweep and downsweep dynamics diverge from one another, disobeying standard bifurcation theory. Nevertheless, we demonstrate universal upsweep and downsweep trajectories for sufficiently slow sweep rates, revealing that the slow trajectories depend essentially on a structural asymmetry parameter, whose effect is negligible for the stationary dynamics. We obtain explicit asymptotic expressions for the universal trajectories and use them to calculate the area of the hysteresis loop enclosed between the upsweep and downsweep trajectories as a function of the asymmetry parameter and the sweep rate.

DOI: 10.1103/PhysRevE.109.044206

I. INTRODUCTION

A key property of dissipative dynamical systems is that bounded trajectories converge towards an attractor, whose properties thus determine the persistent long-term behavior of the system. When the dynamical system depends smoothly on a parameter, the attractor varies smoothly as a function of the parameter, except at special parameter values, where a small parameter variation induces a sharp transition—a bifurcation—in the long-time dynamics of the system. The study of bifurcations is facilitated by the fact that their local structure is universal and captured by a normal-form dynamical system whose dimension is equal to the codimension of the bifurcation [1].

Here we study the persistent dynamics of systems whose parameters are time-dependent and change adiabatically, in the sense that the timescale of parameter variation is much longer than any dynamical timescale. When the system parameters are far from bifurcation points, the convergence to the attractor occurs on a dynamical timescale, and therefore the trajectory of the nonautonomous system follows the time-dependent attractor of the autonomous system with the instantaneous (also called frozen) parameter values, up to an error that tends to zero as the adiabatic timescale tends to infinity. However, bifurcations typically involve the exchange of stability, so the timescale of convergence to the attractor diverges when the system parameters approach a bifurcation point. Therefore, no matter how slowly the parameter is varied, the variation is no longer adiabatic close enough to the bifurcation. Does this observation imply that parameter sweeps are useless as probes of bifurcations? Not necessarily, but the dynamics near a swept bifurcation are qualitatively different than that of an autonomous dynamical system. In particular, the dynamics depend on the direction of the sweep and exhibit hysteresis.

In the context of continuous-time dynamics, the slow sweep of bifurcations has been studied theoretically and experimentally in Refs. [2–6] and other works, demonstrating, in particular, the breakdown of adiabaticity and hysteresis near supercritical bifurcations. A lot of attention has been given to the case where the parameter sweep is periodic, usually produced by oscillatory internal dynamics of a slow degree of freedom, and the system exhibits relaxation oscillation canard cycles [7–10]. Another highly studied effect in adiabatic dynamics is rate-induced tipping, where the system switches from one family of attractors to another family because the adiabatic rate of change is not slow enough [11–14], unlike delayed bifurcations and canard dynamics (sometimes called bifurcation-induced tipping in this context), which occur for an arbitrarily slow change of parameters because the attractor branch ends or becomes unstable.

Here we focus on the adiabatic sweep of bifurcations in the less-studied case of discrete-time dynamical systems, specifically of period-doubling and the closely related pitchfork bifurcations. In experiments, this question arises naturally when studying periodically driven systems, like AC-driven nonlinear electric circuits, which are sampled at drive-period intervals [15–19]. In these cases, parameter sweeping is often used to efficiently extract the attractor for a range of parameter values. The breakdown of adiabaticity and hysteresis in maps undergoing period doubling was demonstrated numerically in Refs. [16,17,20]. A theory of the universal dynamics of maps in the vicinity of a period-doubling bifurcation, based on singular perturbation theory and asymptotic analysis was first put forward in [21], and further developed in Refs. [22,23]. These works introduced the concept of the adiabatic manifold, an attracting submanifold of the extended phase space, on which the dynamics are slow. The theory of Refs. [21–23] is strong and general, but difficult to apply to specific examples, and the adiabatic manifold approach has not yet been used in an experimental context.

This paper aims to derive theoretical results that are directly applicable to experiments and simulations of slow

sweeping of period-doubling bifurcations. For this purpose, we analyze asymptotic trajectories that start sufficiently far from the bifurcation. These trajectories converge on the instantaneous autonomous system attractor well before the control parameter approaches the bifurcation region, where the dynamics of a physical system of interest can be mapped to a universal time-dependent normal form. Moreover, we use the resulting effective dynamics to derive several results, most notably the shape and area of the hysteresis loop in the bifurcation diagram, and its dependence on the adiabatic small parameter, ε, (the sweep rate of the control parameter) that can be easily measured in an experiment or numerical simulation of a given system.

Specifically, we study the trajectory of a one-degree-of-freedom map depending on a single parameter that is adiabatically swept through a supercritical period-doubling bifurcation of a fixed point by considering the trajectory of its second iterate, which has fixed point attractors on both sides of the bifurcation, in Sec. II A. The slow sweep implies that the fixed points vary slightly between subsequent iterations of the map, allowing us to approximate the map by a one-degree-of-freedom normal-form continuous-time flow, as shown in Sec. II B. We next study the dynamics near the bifurcation using the normal-form flow, showing that the universal adiabatic trajectories depend strongly on the asymmetry parameter w that inflicts an overall drift of the fixed points near the bifurcation; the effect of this parameter is negligible in autonomous dynamics. In Secs. III A and III B, we solve the normal-form equations of motion and calculate the upsweep and downsweep trajectories explicitly in the limit where ε, the adiabatic parameter is small. We observe that a key role is played by the parameter $s = \varepsilon^{1/4} w$, which determines the shape of the trajectories, in the sense that adiabatic trajectories with the same s value are related by a scaling transformation. For a fixed map, the shape parameter tends to zero in the adiabatic limit, but the upsweep trajectory does not approach a limiting form. As a consequence, the area of the hysteresis loop has a complicated behavior in the adiabatic limit: its leading asymptotic is $\frac{2}{3}\varepsilon^{1/4}(-\ln(2\pi s^2\sqrt{-\ln(2\pi s^2)}))^{3/4}$, as shown in Sec. III C. The results outlined so far were derived for the adiabatic normal-form map; in Sec. III D, we use the normal-form theory to calculate the adiabatic sweep trajectories of the logistic map in the region of the fundamental period-doubling bifurcation, demonstrating the universality of our theory. Finally, we present our conclusions in Sec. IV.

II. THE EFFECTIVE DYNAMICS

A. The normal-form adiabatic sweep map

We consider nonautonoumous one-degree-of-freedom discrete-time dynamics

$$x_{n+1} = F_n(x_n), \tag{1}$$

with x_n real, viewing F_n as a family of one-variable maps parametrized by the integer n. We assume that the dynamics of (1) is adiabatic in the sense that the difference between the maps F_n for consecutive values of the parameter is small and that there is a range of n values around zero where the maps F_n have a fixed point $y_0(n) = F_n(y_0(n))$ that undergoes

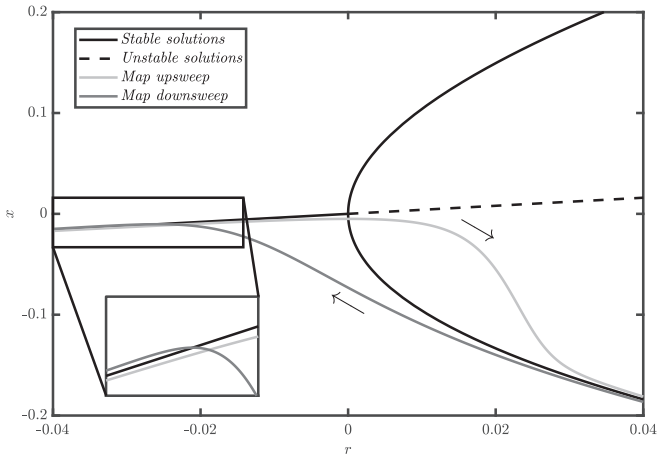

FIG. 1. Instantaneous fixed points (full black lines, stable, and broken black line, unstable) and adiabatic sweep trajectories (gray) of the normal-form family of maps $F_{r,u}$ [defined in (3)], as a function of the parameter r, choosing $u = wr$, $w = 0.4$. Instantaneous fixed points are solutions of $F_{r,u}(y) = y$, showing the standard supercritical pitchfork structure at $r = 0$. Adiabatic trajectories are trajectories of (4) with parameters varying according to (5) with $\varepsilon = 10^{-4}$, and positive and negative sign choice in (5) yielding the upsweep (pale gray) and downsweep (dark gray) trajectory, respectively. Note that since the adiabatic trajectories are shown as a function of the instantaneous value of the parameter r that changes by $\pm\varepsilon$ each time step, the spacing between consecutive points is so small that they overlap in the figure, obscuring the discrete nature of the map dynamics and motivating the continuum approximation, and that time increases from right to left for the downsweep trajectory, as indicated by the arrows. Adiabatic dynamics was calculated starting from a large negative initial time, allowing the trajectory to reach the close vicinity of one of the stable fixed points, and making it independent of the initial value of x. We observe that the up- and downsweep trajectories are different, forming a hysteresis loop whose width and height are proportional to $\varepsilon^{1/2}$ and $\varepsilon^{1/4}$, respectively, up to logarithmic corrections. For r values outside this interval, the adiabatic trajectories follow one of the stable instantaneous fixed points up to small corrections shown in the inset.

a supercritical pitchfork bifurcation at $n = 0$. For adiabatic upsweep, this means that when $n < 0$, y_0 is linearly stable $|\partial_x F_n(y_0(n))| < 1$, and when $n > 0$, y_0 becomes unstable $\partial_x F_0(y_0(n)) > 1$, and two stable fixed points $y_\pm(n)$ appear. Far from the bifurcation, the slow parametric variation of F_n implies that x_n is attracted to a stable fixed point, $y_0(n)$ if $n < 0$ and one of $y_\pm(n)$ if $n > 0$, but near the bifurcation, adiabaticity breaks down no matter how slow the variation of F_n is, and the dynamics follows the universal upsweep trajectory instead. Adiabatic downsweep is similar except that the roles of negative and positive n are reversed; the upsweep and downsweep trajectories, shown for a particular choice of F_n in Fig. 1 overlayed with the instantaneous fixed points, are universal in the sense that they do not depend on the details of the family of maps, as explained in detail below. The analysis of these dynamics also covers the case of adiabatic sweeping through a period-doubling bifurcation, because when a map G period-doubles, its second iterate $F \equiv G^2$ undergoes a pitchfork bifurcation [1]. It is preferable to start with the adiabatic

analysis of the pitchfork-bifurcation family, because, unlike the period-doubling family, its maps have a stable fixed point for every n, facilitating the continuum model approximation of Sec. II B below.

The universal dynamics in the vicinity of the pitchfork bifurcation is studied using a normal-form family of maps. A normal-form family of maps depending on the control parameter r, whose autonomous dynamics undergoes a pitchfork bifurcation at $r = 0$, is given by [1]

$$F_r(x) = (1 + r)x - x^3, \tag{2}$$

with fixed points $y_0 = 0$ and, for $r > 0$, $y_\pm = \pm\sqrt{r}$. When the dynamics near a pitchfork bifurcation is autonomous, y_0 can always be shifted to zero by a change of coordinates, but for the adiabatic dynamics of (1), y_0 varies with the parameter and its time dependence must be taken into account; for this reason, we have to use a two-parameter normal-form map

$$F_{r,u}(x) = u + (1 + r)(x - u) - (x - u)^3 \tag{3}$$

with $y_0 = u$. For adiabatic dynamics, we let the parameters depend on time so we choose the normal-form adiabatic map

$$x_{n+1} = F_n^{\mathrm{NF}}(x_n) = F_{r_n,u_n}(x_n). \tag{4}$$

Adiabatic sweep means that the timescale of variation of the parameters r and u is much longer than a single time step of the map, so the paramater steps $r_{n+1} - r_n$, $u_{n+1} - u_n$ are of order ε, $0 < \varepsilon \ll 1$. Our goal is to derive the universal part of the adiabatic sweep trajectories, which, like the universal trajectories of autonomous maps, takes place for sufficiently small r, even though it consists of many time steps; in particular, we show below that the sweep trajectories follow closely one of the stable fixed points except in an order-$\sqrt{\varepsilon}$-width interval of parameter values, consisting of $O(\varepsilon^{-1/2})$ time steps. In particular, the relevant interval of parameters is small, so we may approximate r_n, u_n in it by linear functions, and since by shifting x and n we can make $r_0 = u_0 = 0$, we let

$$r_n = \pm\varepsilon n, \quad u_n = \varepsilon w n, \tag{5}$$

where w is an order-one real number that parametrizes the overall drift rate of the fixed points of the system. Equations (3)–(5) define the normal-form adiabatic sweep model. A positive (negative) sign in (5) generates adiabatic upsweep (downsweep) trajectories, respectively.

The universal sweep trajectories are obtained by starting at some negative n with sufficiently large absolute value, so the trajectories approach one of the stable instantaneous fixed points of F well before n changes signs, and iterating the map until n becomes positive and large enough to observe the eventual convergence to a different branch of instantaneous fixed points that become stable for positive n. Figure 1 shows example upsweep and downsweep trajectories of the map F^{NF} with parameters evolving according to (5), choosing $\varepsilon = 10^{-4}$, $w = 0.4$, overlayed with the instantaneous fixed points of the map. The sign of w breaks the sign-flip symmetry of the pitchfork bifurcation, and in the positive-w case shown in Fig. 1, the upsweep trajectory remains below y_0, eventually converging to y_-, which is used as the starting point of the downsweep trajectory. Our next goal is to study the adiabatic sweep trajectories and the hysteresis loop using a continuum approximation.

B. Continuous-time dynamics approximation

The continuum model approximation starts from the observation that since the parameters of the normal-form map F^{NF} change slowly, its fixed points change slowly, and therefore if x_n is close to a fixed point of F_n^{NF}, then x_{n+1} is close both to x_n and to a fixed point of F_{n+1}^{NF}. It follows that after the initial transient, the adiabatic trajectory approaches a branch of instantaneous stable fixed points and remains close to an instantaneous fixed point throughout its evolution. Adopting this view, substituting (3) and (5) in (4), and subtracting x_n from both sides,

$$x_{n+1} - x_n = \pm\varepsilon n(x_n - \varepsilon w n) - (x_n - \varepsilon w n)^3, \tag{6}$$

that by letting $y_n = x_n - \varepsilon w n$ is simplified to

$$y_{n+1} - y_n = \pm\varepsilon n y_n - y_n^3 - \varepsilon w. \tag{7}$$

The steps $x_{n+1} - x_n$ are therefore small, so we can view n as a real variable and approximate $x_{n+1} - x_n \sim dx/dn$, and obtain the continuum version of the adiabatic sweep normal-form dynamics

$$\frac{dy}{dn} = \pm\varepsilon n y - y^3 - \varepsilon w; \tag{8}$$

as before a positive (negative) sign choice in the equation of motion corresponds to upsweep (downsweep) dynamics, respectively. In Eq. (7), the only explicit time dependence is in the linear term on the right-hand side. The adiabatic parameter can be eliminated from this term by transforming to the slow time variable $t = \sqrt{\varepsilon} n$, obtaining

$$\frac{dy}{dt} = \pm t y - \frac{y^3}{\sqrt{\varepsilon}} - \sqrt{\varepsilon} w. \tag{9}$$

Since the variable t describes the adiabatic sweep of map parameters, we see that the range of parameter values near the bifurcation where the sweep trajectory fails to follow one of the fixed points is of order $\sqrt{\varepsilon}$, as seen in Fig. 1; in particular, this interval is small, justifying the linear approximation to the time dependence of the map parameters made in (5), and giving rise to the universal shape of the adiabatic trajectories.

The validity of (9) as an approximation to (4) is checked in Fig. 2, which shows a comparison between the numerically calculated trajectories of the continuous-time equation (9) and those of the discrete time map dynamics in Eq. (4). As expected, we observe that the difference between the continuum and discrete trajectories is small, and decreases with the value of the adiabatic parameter ε.

Next, we want to identify the characteristic scale of y for small ε. It turns out that there are two regimes in (9) with different characteristic scales. When $t < 0$ for the upsweep and $t > 0$ for the downsweep trajectory, y approaches

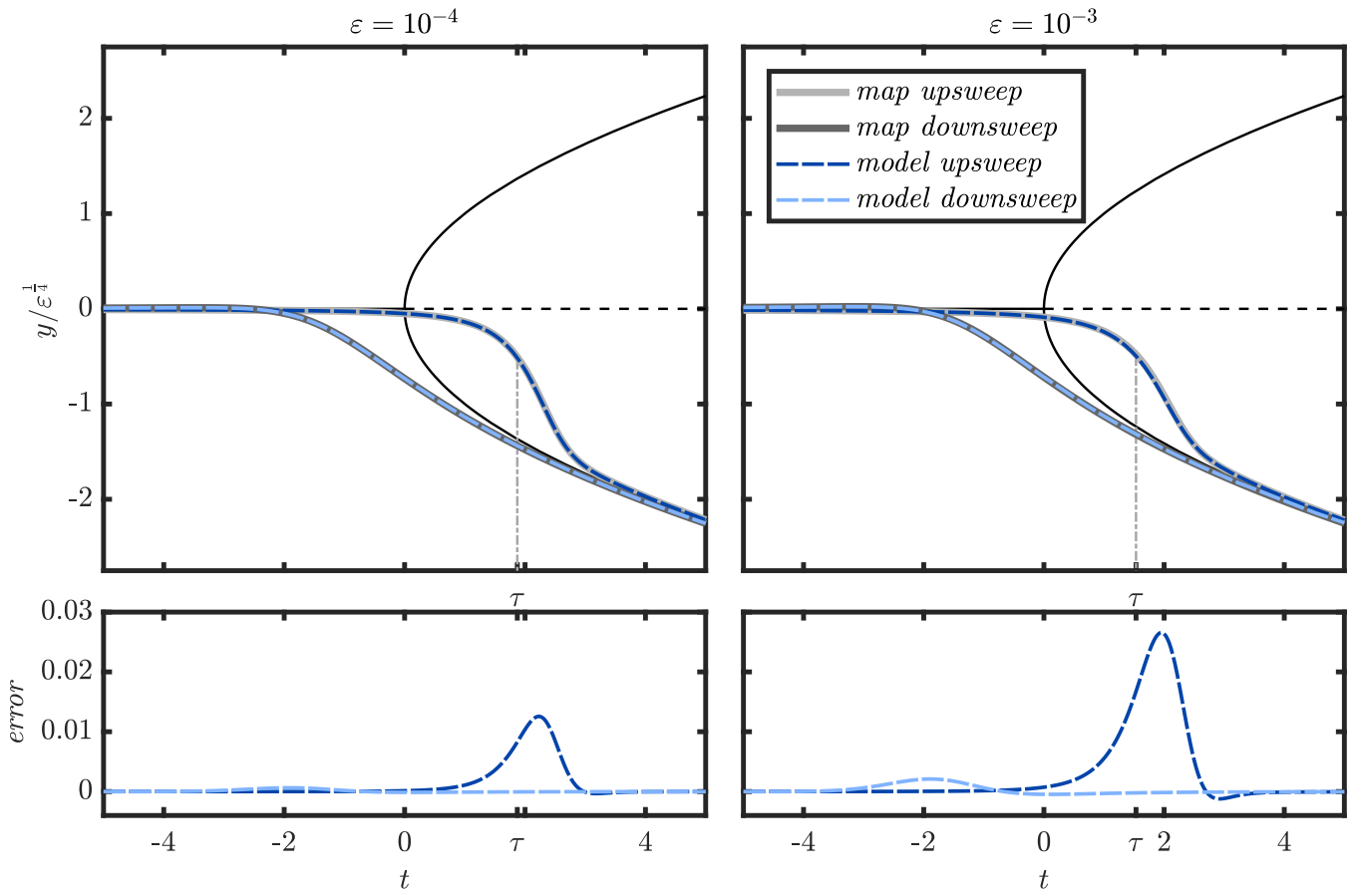

FIG. 2. Top: Continuum model trajectories from numerical solutions of Eq. (9) in turquoise (thin dashed dark gray) and blue (thin dashed pale gray) for upsweep and downsweep, respectively, overlayed on the trajectories of the map (4) (after transformation from n and x to t and $y/\varepsilon^{1/4}$) in pale (upsweep) and dark (downsweep) gray, alongside the instantaneous fixed points of the map in filled (stable) and dashed (unstable) black. Bottom: The difference between the trajectories of the continuum model and the map, showing that as $\varepsilon \to 0$ the trajectories of the continuous- and discrete-time systems approach each other. Here we used $\varepsilon = 10^{-4}$, $w = 0.4$ ($s = 0.04$) in the left panels, and $\varepsilon = 10^{-3}$, $w = 0.4$ ($s = 0.07$), in the right panels.

0, so $y \sim \sqrt{\varepsilon}$, and the cubic term is negligible. In this time interval, which will be referred to as the small-y regime, the appropriate scaling is $y = \sqrt{\varepsilon} y_s$, and the equation of motion becomes

$$\frac{dy_s}{dt} = \pm t y_s - w - \sqrt{\varepsilon} y_s^3. \tag{10}$$

On the other hand, when $\pm t > 0$, y approaches one of the branches $\pm\varepsilon^{1/4}\sqrt{|t|}$, so $y \sim \varepsilon^{1/4}$, and the term proportional to w is negligible. In this time interval, which will be referred to as the large-y regime, the appropriate scaling is $y = \varepsilon^{1/4} y_l$, and the equation of motion becomes

$$\frac{dy_l}{dt} = \pm t y_l - y_l^3 - \varepsilon^{1/4} w. \tag{11}$$

The crossover between the two regimes occurs at different times for the upsweep and downsweep trajectories which we will identify next, and then use to calculate the crossover trajectories.

The form (11) of the effective dynamics equation of motion makes it clear that the only dimensionless parameter in the adiabatic dynamics is $s = \varepsilon^{1/4} w$; since s determines the trajectories $y(t)$ up to scaling, we will refer to it as the shape parameter. Note, however, that unlike w, s tends to zero in the adiabatic limit, so the limit $\varepsilon \to 0$ with s fixed is not appropriate for studying the adiabatic sweep problem. Furthermore, this is a singular limit, in the sense that the adiabatic trajectories and the hysteresis loop do not converge to a well-defined shape.

III. THE ADIABATIC TRAJECTORIES

We seek solutions of the adiabatic equation of motion (9) or its equivalent (10) and (11), that start far from the bifurcation at some $t < 0$, and end far on the other side of the bifurcation for $t > 0$. Far from the bifurcation point, the adiabatic sweep trajectories track a stable instantaneous fixed point of (6) up to small deviations, so we seek solutions that start close to these points for sufficiently negative t, studying upsweep and downsweep trajectories separately.

A. Adiabatic upsweep

Starting with $t < 0$, $|t|$ of order one or larger in the small-y regime, y_s is of order one, and the nonlinear term is negligible. In this approximation, the solution of (10) (choosing the

positive sign for upsweep) that tends to 0 as $t \to -\infty$ is

$$y_{s\uparrow}(t) = -w\int_{-\infty}^{t} e^{\frac{1}{2}(t^2-(t')^2)}dt' = -w\sqrt{\frac{\pi}{2}}e^{\frac{1}{2}t^2}\,\mathrm{erfc}\left(-\frac{\mathrm{t}}{\sqrt{2}}\right), \tag{12}$$

where erfc stands for the complementary error function [24]. The approximation remains valid as long as $|y_{s\uparrow}| \ll \varepsilon^{-1/4} \Leftrightarrow |y_\uparrow| \ll \varepsilon^{1/4}$; since $\mathrm{erfc}(t) \sim e^{-t^2}/(\sqrt{\pi}t)$ as $t \to \infty$, it follows that (12) remains valid for all negative t, and since $\mathrm{erfc}(t) \to 2$ as $t \to -\infty$, also for positive t such that $e^{\frac{1}{2}t^2} \ll \varepsilon^{-1/4}$. For times later than this range, the nonlinear term in Eq. (9) becomes important, so the scaling of the large-y regime is applicable, while the term proportional to w becomes negligible. When this term is neglected, (11) becomes a Bernoulli equation, whose general solution is

$$y_{l\uparrow}(t) = \pm\frac{e^{t^2/2}}{\sqrt{c_1 + \sqrt{\pi}\,\mathrm{erfi}(t)}}, \tag{13}$$

where $\mathrm{erfi}(t) = -i(1-\mathrm{erfc}(it))$, and c_1 is an arbitrary constant of integration. For t large and positive, $\mathrm{erfi}(t) \sim e^{t^2}/(\sqrt{\pi}t)$, so $y_l(t) \to \pm\sqrt{t}$ for all values of c_1; the constant has to be determined by matching the right-hand side of Eq. (13) with that of Eq. (12).

For this purpose, we note that w is negligible in Eq. (11) as long as $|y_{l\uparrow}| \gg \varepsilon^{1/4} \Leftrightarrow |y_\uparrow| \gg \sqrt{\varepsilon}$, so there is an overlap interval $\sqrt{\varepsilon} \ll y_\uparrow \ll \varepsilon^{1/4}$, where both Eq. (12) for the small-y regime and Eq. (13) for the large-y regime are valid. In this interval, $y_{s\uparrow}(t) \sim -\sqrt{2\pi}\,we^{\frac{1}{2}t^2}$ and for this asymptote to match Eq. (13), we must choose $c_1 \gg \mathrm{erfi}(t)$ in the interval to ensure that $y_{l\uparrow}(t) \sim \pm c_1^{-1/2}e^{\frac{1}{2}t^2}$. Recalling that $y_{s\uparrow} = \varepsilon^{-1/4}y_{l\uparrow}$, it follows that the two asymptotes match if

$$c_1 = (2\pi w^2)^{-1}\varepsilon^{-1/2} \tag{14}$$

and the ambiguous sign in (13) is chosen to match the sign of $-w$.

In summary, we obtain the all-time aymptotic approximation for the adiabatic upsweep trajectory:

$$y_\uparrow(t) = \begin{cases} -\sqrt{\varepsilon}w\sqrt{\frac{\pi}{2}}e^{t^2/2}\,\mathrm{erfc}\left(-\frac{\mathrm{t}}{\sqrt{2}}\right) & t \leqslant 0,\ \text{or } t > 0 \text{ and } e^{\frac{1}{2}t^2} \ll \varepsilon^{-1/4} \quad \text{(small } y\text{)} \\ -\mathrm{sign(w)}\dfrac{\varepsilon^{1/4}\mathrm{e}^{\mathrm{t}^2/2}}{\sqrt{(2\pi\,\mathrm{w}^2)^{-1}\varepsilon^{-1/2} + \sqrt{\pi}\,\mathrm{erfi(t)}}} & t > 0 \text{ and } 1 \ll e^{\frac{1}{2}t^2} \quad \text{(large } y\text{)}. \end{cases} \tag{15}$$

We check that the small- and large-y asymptotics agree in their common interval of validity, and that $c_1 \gg \mathrm{erfi(t)}$ holds in this interval. It is useful to express the result also in terms of the shape parameter $s = \varepsilon^{1/4}w$:

$$y_\uparrow(t) = -\varepsilon^{1/4}\begin{cases} s\sqrt{\frac{\pi}{2}}e^{t^2/2}\,\mathrm{erfc}\left(-\frac{\mathrm{t}}{\sqrt{2}}\right) & t \leqslant 0,\ \text{or } t > 0 \text{ and } e^{\frac{1}{2}t^2} \ll 1/s \quad \text{(small } y\text{)} \\ \mathrm{sign(s)}\dfrac{\mathrm{e}^{\mathrm{t}^2/2}}{\sqrt{(2\pi\,\mathrm{s}^2)^{-1} + \sqrt{\pi}\,\mathrm{erfi(t)}}} & t > 0 \text{ and } 1 \ll e^{\frac{1}{2}t^2} \quad \text{(large } y\text{)}. \end{cases} \tag{16}$$

B. Adiabatic downsweep

Starting with $t < 0$, $|t|$ of order one or larger in the large-y regime, $|y_l|$ is comparable with $\sqrt{-t}$, and the term proportional to w is initially negligible. In this approximation, the solutions of Eq. (11) (choosing the negative sign for downsweep) that approach $\pm\sqrt{-t}$ as $t \to -\infty$ are

$$y_{l\downarrow}(t) = \frac{\pm e^{-t^2/2}}{\pi^{1/4}\sqrt{\mathrm{erfc}(-\mathrm{t})}}, \tag{17}$$

respectively. As in the case of Eq. (13), this approximation remains valid as long as $|y_{l\downarrow}| \gg \varepsilon^{1/4}$, which here holds for all negative t, and for positive t small enough that $e^{-t^2/2} \gg \varepsilon^{1/4}$. For later times, the trajectory is in the small-y regime, and we can use (10) without the nonlinear term, whose general solution is

$$y_{s\downarrow}(t) = e^{-t^2/2}\left(c_2 - w\sqrt{\frac{\pi}{2}}\,\mathrm{erfi}\left(\frac{t}{\sqrt{2}}\right)\right), \tag{18}$$

valid when $|y_{s\downarrow}| \ll \varepsilon^{-1/4}$. In the overlap interval $\sqrt{\varepsilon} \ll |y_\downarrow| \ll \varepsilon^{1/4}$, $c_2 \gg \mathrm{erfi}(\frac{\mathrm{t}}{\sqrt{2}})$, and $\mathrm{erfc(t)} \sim 2$, so the asymptotes match if we choose

$$c_2 = \pm\varepsilon^{-1/4}/(\sqrt{2}\pi^{1/4}). \tag{19}$$

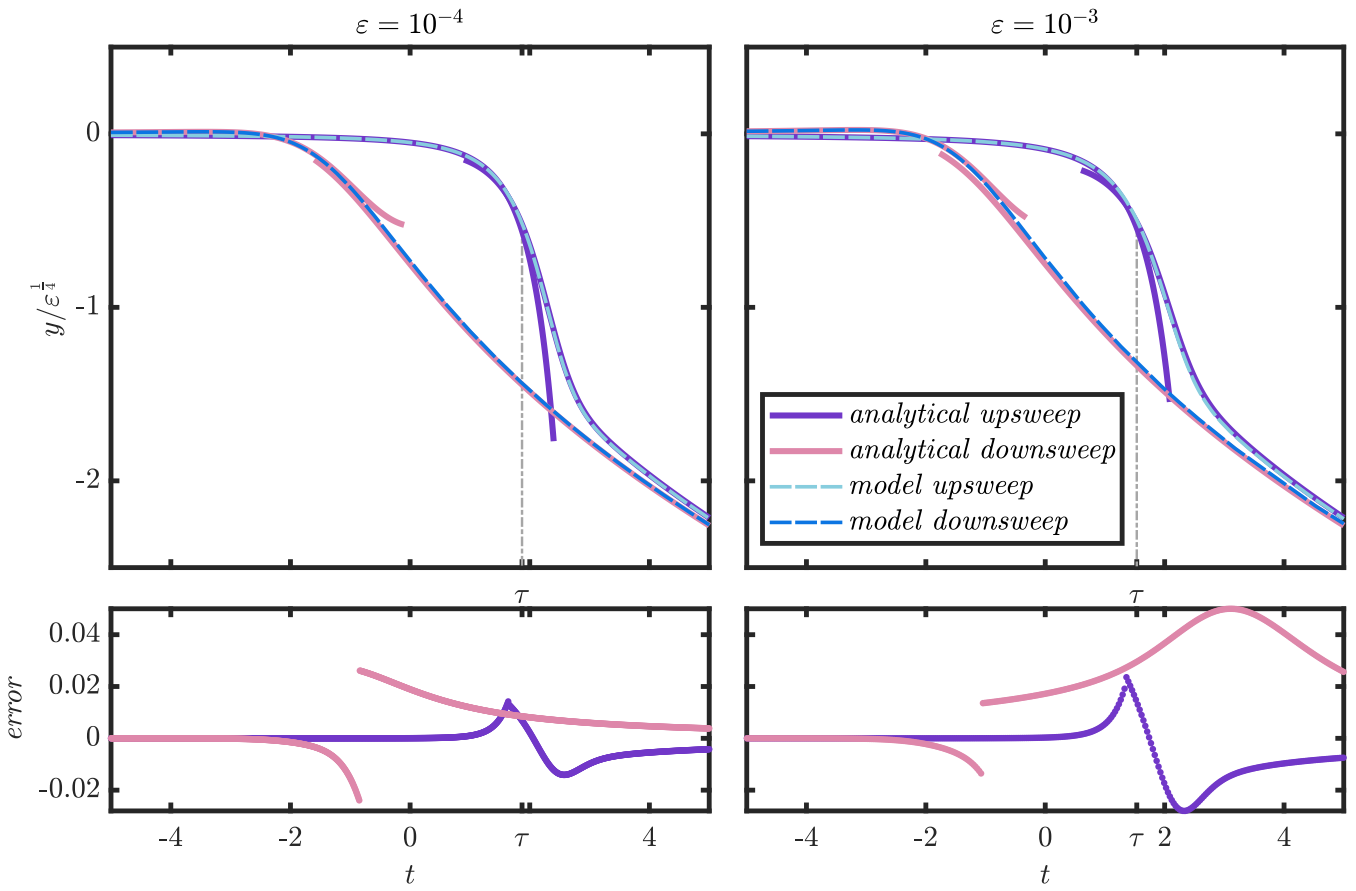

FIG. 3. Top: The asymptotic approximations of the adiabatic trajectories given in Eqs. (16) and (21) in purple (dark gray) and violet (pale gray) for upsweep and downsweep, respectively, overlayed with the numerically calculated continuum model trajectories of Eq. (9) in turquoise (thin dashed light gray) and blue (thin dashed dark gray) for upsweep and downsweep, respectively. The asymptotic approximations given in Eqs. (16) and (21) are shown each with two curves corresponding to the small-y (left) and large-y (right) regimes, in their overlapping intervals of validity. The breakout time τ, defined in Sec. III C, is marked in a dotted black line. Bottom: The difference between the asymptotic approximation and the numerically calculated trajectories. In the overlap interval where both the early- and late-time asymptotes are valid, the smaller error in absolute value is shown. As in Fig. 2, $\varepsilon = 10^{-4}$, $w = 0.4$ ($s = 0.04$) in the left panels, and $\varepsilon = 10^{-3}$, $w = 0.4$ ($s = 0.07$) in the right panels. As expected, the error in the asymptotic approximations decreases with decreasing ε.

The all-time asymptotic approximation for the downsweep trajectory is therefore

$$y_{\downarrow}(t) = \begin{cases} \dfrac{\pm\varepsilon^{1/4} e^{-t^2/2}}{\pi^{1/4}\sqrt{\operatorname{erfc}(-t)}} & t \leqslant 0, \text{ or } t > 0 \text{ and } e^{\frac{1}{2}t^2} \ll \varepsilon^{-1/4} \quad \text{(large } y\text{)} \\ \sqrt{\varepsilon} e^{-t^2/2}\left(\pm \dfrac{\varepsilon^{-1/4}}{\sqrt{2}\pi^{1/4}} - w\sqrt{\dfrac{\pi}{2}}\operatorname{erfi}\left(\dfrac{t}{\sqrt{2}}\right)\right) & t > 0 \text{ and } 1 \ll e^{\frac{1}{2}t^2} \quad \text{(small } y\text{)} \end{cases} \tag{20}$$

or

$$y_{\downarrow}(t) = \varepsilon^{1/4} \begin{cases} \dfrac{\pm e^{-t^2/2}}{\pi^{1/4}\sqrt{\operatorname{erfc}(-t)}} & t \leqslant 0, \text{ or } t > 0 \text{ and } e^{\frac{1}{2}t^2} \ll 1/s \quad \text{(large } y\text{)} \\ e^{-t^2/2}\left(\pm \dfrac{1}{\sqrt{2}\pi^{1/4}} - s\sqrt{\dfrac{\pi}{2}}\operatorname{erfi}\left(\dfrac{t}{\sqrt{2}}\right)\right) & t > 0 \text{ and } 1 \ll e^{\frac{1}{2}t^2} \quad \text{(small } y\text{)}, \end{cases} \tag{21}$$

in terms of the shape parameter.

Figure 3 shows a comparison between the asymptotic approximations given in Eqs. (16) and (21) and numerical solutions of the continuum model (9), confirming the validity of the early and late asymptotic approximations in the expected intervals and the overlap of the validity intervals.

C. The hysteresis loop

The breakdown of adiabaticity near the bifurcation point breaks time-reversal symmetry, yielding essentially different dynamics in the upsweep and downsweep directions. The most important expression of this difference is the delay τ

between the time that the control parameter r sweeps through the bifurcation point in the upward direction, and the time where the map trajectory approaches the attractor near $\pm\varepsilon^{1/4}\sqrt{t}$.

A convenient definition for the upsweep breakout time τ is the time where the upsweep trajectory $y_\uparrow$ reaches the midway point $\pm\varepsilon^{1/4}\sqrt{t}/2$ between the stable and unstable branches. For this t, we can use the late-time asymptotic Eq. (16), approximating $\mathrm{erfi}(t) \sim e^{t^2}/(\sqrt{\pi}t)$, to obtain

$$\frac{\sqrt{\tau}}{2} = \frac{\sqrt{\tau}}{\sqrt{(2\pi s^2)^{-1}\tau e^{-\tau^2}+1}} \Rightarrow 2\pi s^2 \tau e^{\tau^2} = \frac{1}{3} \Rightarrow \tau \sim \sqrt{-\ln(6\pi s^2)} \tag{22}$$

in the adiabatic limit where $s \to 0$; note that τ diverges logarithmically in this limit.

The breakout time τ is a measure of the temporal width of the upsweep-downsweep hysteresis loop, whose height is therefore $\sim\varepsilon^{1/4}\sqrt{\tau}$, yielding the estimated area $\varepsilon^{1/4}\tau^{3/2} \sim \varepsilon^{1/4}(-\ln s)^{3/4}$ for the area of the loop in the y,t space, or $\varepsilon^{3/4}(-\ln s)^{3/4}$ in the x,r space.

To obtain a more precise approximation, we define the normalized loop area

$$H = \frac{1}{\varepsilon^{1/4}}\left|\int_{-\infty}^{\infty}(y_\downarrow(-t)-y_\uparrow(t))dt\right| \tag{23}$$

that is a function of s only. It follows from the preceding arguments that H diverges in the limit $s \to 0$; our goal is to identify the form of this divergence, and in this view we can subtract from H contributions that remain finite in this limit. Thus, we can restrict the domain of integration to the interval $0 \leqslant t < \infty$ and use the early-time approximation $\pm\varepsilon^{1/4}\sqrt{-t}$ for $y_\downarrow(t)$ and the late-time approximation $\pm\varepsilon^{1/4}\sqrt{t/(1+(2\pi s^2)^{-1}te^{-t^2})}$ for $y_\uparrow(t)$, so as $s \to 0$,

$$H \sim \int_0^\infty \sqrt{t}\left(1-\frac{1}{\sqrt{1+(2\pi s^2)^{-1}te^{-t^2}}}\right)dt. \tag{24}$$

As observed above, for $t \lesssim \tau$, the second term in the integrand is much smaller than the first, but for $t \gg \tau$ the two terms in the integrand cancel, so the integration is effectively cut off at τ from above. An analysis of the asymptotic approximation of the area, outlined in the Appendix, shows that in the limit $s \to 0$,

$$H \sim \frac{2}{3}\left(\ln\left(\frac{\sqrt{-\ln(2\pi s^2)}}{2\pi s^2}\right)\right)^{3/4} + H_0, \tag{25}$$

where H_0 is an indeterminate constant; least squares fitting yields $H_0 \approx 0.8853$

Figure 4 compares $H(s)$, calculated in four ways: (a) directly from the adiabatic sweep trajectories of the normal-form map (4), (b) from the numerical solutions of the continuum model (9), (c) from the asymptotic approximations for the sweep trajectories (16) and (21), and (d) from the asymptotic approximation to H (25), regarding H_0 as a fit parameter. The values obtained by the four methods converge in the adiabatic limit $s \to 0$.

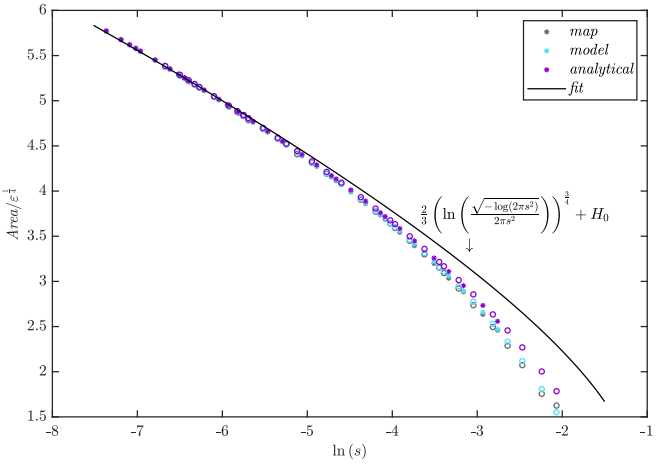

FIG. 4. The area enclosed within the hysteresis loop in the t,y plane divided by $\varepsilon^{1/4}$ versus $\ln(s)$ (natural logarithm of the shape parameter). The area is calculated in four different ways: using the adiabatic trajectories of the normal-form map in gray, the numerically calculated trajectories of the continuum model Eq. (8) in turquoise (light gray), the asymptotic approximations of the continuum trajectories in purple (dark gray), and the explicit asymptotic approximation of the area (25) in black, using H_0 as a fit parameter. Circle (respectively, asterisk) symbols are used for cases where the map trajectories were calculated for $w = 0.4$ (respectively, $w = 0.2$).

D. Universality of the adiabatic trajectories: The logistic map

As argued above, the adiabatic sweep trajectories that we derived and the resultant hysteresis loop are universal; they capture the shape of any sufficiently slow sweep trajectories of a map through a period-doubling or pitchfork bifurcation, sufficiently close to the bifurcation point. We next demonstrate this claim for the case of the logistic map

$$x_{n+1} = L_n(x_n), \quad L_n(x) = \left(3 \pm \frac{1}{2}\varepsilon n\right)x(1-x), \tag{26}$$

with $\varepsilon > 0$ small and with positive and negative sign choice corresponding to upsweep and downsweep trajectories (respectively) as above. Note that we parametrize $L_n(x)$ such that it passes through the fundamental period-doubling bifurcation of the logistic map at $n = 0$. As discussed above, the universal trajectories in Eqs. (15) and (20) are adiabatic asymptotic approximants to trajectories of $M_n = L_n^2$, which undergoes a supercritical pitchfork bifurcation at $n = 0$; meanwhile, trajectories of M_n are adiabatic approximants of trajectories of $L_n \circ L_{n-1}$.

To bring the second iterate of the logistic map to normal form, we apply a linear transformation, shifting the bifurcation point to zero and stretching the map vertically so the positive-n outer instantaneous fixed points of the map are at the standard $\pm\sqrt{\varepsilon n} + O(\varepsilon)$. This transformation produces the stretched and shifted map $N_n = \sqrt{18}(M_n(\frac{x}{\sqrt{18}} + \frac{2}{3}) - \frac{2}{3})$; the instantaneous inner fixed point of N_n is at $\varepsilon n/\sqrt{18} + O(\varepsilon^2)$, and thus $w = 1/\sqrt{18}$ in this example.

Figure 5 shows a comparison between the adiabatic sweep trajectories of N_n and those of the normal-form map F_n of Eq. (4). The figure confirms that for small enough r and ε,

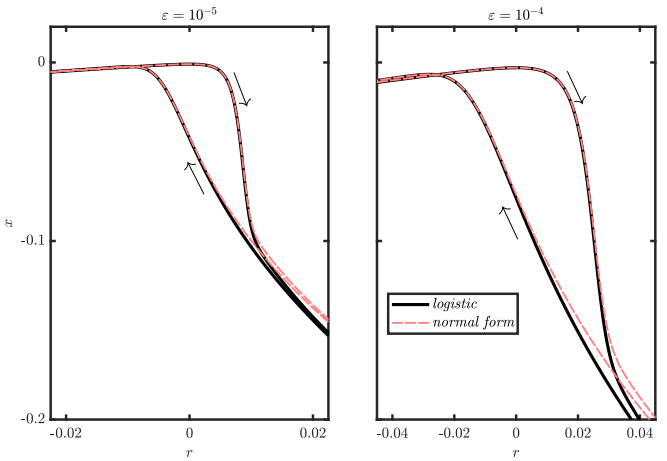

FIG. 5. Adiabatic sweep trajectories of the shifted and stretched second iterate of the logistic map N_n in black and of the normal map F_n in red (thin dashed gray) for two values of the adiabatic parameter (sweep rate) ε. The agreement is good and improves for decreasing ε.

the adiabatic logistic map indeed behaves like the universal map.

IV. DISCUSSION AND CONCLUSIONS

Bifurcations in autonomous dynamical systems are important because they mark a qualitative change in the long-term behavior of the system. The study of bifurcations is facilitated by the transformation to a normal form, which allows one to calculate the trajectories of the system near the bifurcation. Since the normal form has a universal structure, the dynamics near the bifurcation are universal.

Here we analyzed the dynamics of an adiabatically time-dependent map that is swept past a period-doubling or pitchfork bifurcation. The first main result of this analysis is the development of the adiabatic normal form for this class of bifurcations from which it follows that the universal adiabatic sweep dynamics depends on a structural asymmetry parameter, which is irrelevant for the autonomous bifurcation analysis. The shape of the adiabatic sweep trajectories is determined, up to scaling, by the shape parameter, a combination of the asymmetry parameter and the adiabatic small parameter (which is the sweep rate). Thus, even though all autonomous period-doubling and pitchfork bifurcations have the same structure after appropriate scaling, there is a one-parameter family of structures of adiabatic sweeping trajectories of these bifurcations.

Our second main result is the complete asymptotics of the up- and downsweep adiabatic trajectories, explicitly expressed in terms of error functions. In both directions, the trajectory initially follows closely a branch of the instantaneous stable fixed points of the map, but opens an increasing gap from it upon approaching the bifurcation, before finally breaking back toward a stable branch after leaving the bifurcation region. The breakdown of adiabaticity at the bifurcation is the source of asymmetry between the up- and downsweep trajectories that gives rise to hysteresis.

On the basis of these explicit asymptotic expressions, we next calculated the area of the hysteresis loop enclosed between the upsweep and downsweep trajectories. We showed that even though the adiabatic-trajectory shape parameter tends to zero in the adiabatic limit, the hysteresis loop itself does not converge to a well-defined shape in this limit and, as a consequence, the area of the loop has a complicated logarithmic adiabatic asymptote. Finally, as an application of our results, we showed that the universal sweep trajectories correctly capture the dynamics of the logistic map with an adiabatically varying parameter in the region of the fundamental period-doubling bifurcation.

The results of this paper are geared to be useful for the analysis of adiabatic sweep experiments and simulations. While the breakdown of adiabaticity implies that the autonomous dynamics close to a bifurcation and, in particular, the location of the bifurcation point itself, can never be faithfully reproduced by a finite speed sweeping, full information about the bifurcation structure can be extracted from the sweep trajectories, namely, a fit of the experimental trajectories with the universal ones would yield both the location of the bifurcation point and the values of the map parameters at the bifurcation, from which it is possible to reconstruct the bifurcation diagram of the autonomous map.

APPENDIX: ASYMPTOTIC APPROXIMATION OF THE AREA OF THE HYSTERESIS LOOP

In this Appendix, we derive an asymptotic approximation for the integral

$$H_a = \int_0^\infty \sqrt{t}\left(1 - \frac{1}{\sqrt{1+ate^{-t^2}}}\right)dt \;= \frac{2}{3}\int_0^\infty \left(1 - \frac{1}{\sqrt{1+at^{2/3}e^{-t^{4/3}}}}\right)dt \tag{A1}$$

in the limit $a = (2\pi s^2)^{-1} \to \infty$. Changing the variable to $x = e^{-t^{4/3}}$, we get

$$H_a = \frac{1}{2}\int_0^1 \left(1 - \frac{1}{\sqrt{1+ax\sqrt{-\ln x}}}\right)\frac{dx}{x(-\ln x)^{1/4}} = \int_0^1 \frac{a(-\ln x)^{1/4}dx}{2\sqrt{1+ax\sqrt{-\ln x}}\left(\sqrt{1+ax\sqrt{-\ln x}}+1\right)}. \tag{A2}$$

To estimate this integral, note that for a given $a \gg 1$, and x which is not too small, $ax\sqrt{-\ln x} \gg 1$, and for such x,

$$\frac{a(-\ln x)^{1/4}}{2\sqrt{1+ax\sqrt{-\ln x}}\left(\sqrt{1+ax\sqrt{-\ln x}}+1\right)} \sim \frac{1}{2x(-\ln x)^{1/4}}, \tag{A3}$$

which is logarithmically divergent for small x.

On the other hand, for sufficiently small x, $ax\sqrt{-\ln x} \ll 1$, and for such x, the integrand in Eq. (A2) is close to $a(-\ln x)^{1/4}/4$, which is integrable at 0. The crossover between the two limits occurs for $x \sim 1/(a\sqrt{\ln a})$, so it is advantageous to express

$$H_a = \left(\int_0^{k/(a\sqrt{\ln a})} + \int_{k/(a\sqrt{\ln a})}^1\right) \frac{a(-\ln x)^{1/4}dx}{2\sqrt{1+ax\sqrt{-\ln x}}(\sqrt{1+ax\sqrt{-\ln x}}+1)}, \tag{A4}$$

with k an order-one number. The small-x integral is $\sim\frac{k}{4}(\ln a)^{-1/2}(\ln(a\sqrt{\ln a}/k))^{1/4}$, and can be neglected in the limit $a \to \infty$, and we can let k be large enough that the estimate (A3) is valid for all x in the larger-x integral, obtaining, finally,

$$H_a \sim \int_{k/(a\sqrt{\ln a})}^1 \frac{1}{2x(-\ln x)^{1/4}} \sim \frac{2}{3}(\ln(a\sqrt{\ln a}))^{3/4}. \tag{A5}$$

[1] S. Wiggins, *Introduction to Applied Nonlinear Dynamical Systems and Chaos*, 2nd ed., Texts in Applied Mathematics, Vol. 2 (Springer, New York, 2003).

[2] N. R. Lebovitz and R. J. Schaar, Exchange of stabilities in autonomous systems, Stud. Appl. Math. **54**, 229 (1975).

[3] R. Haberman, Slowly varying jump and transition phenomena associated with algebraic bifurcation problems, SIAM J. Appl. Math. **37**, 69 (1979).

[4] T. Erneux and P. Mandel, Imperfect bifurcation with a slowly-varying control parameter, SIAM J. Appl. Math. **46**, 1 (1986).

[5] P. Mandel and T. Erneux, The slow passage through a steady bifurcation: delay and memory effects, J. Stat. Phys. **48**, 1059 (1987).

[6] D. Premraj, K. Suresh, T. Banerjee, and K. Thamilmaran, An experimental study of slow passage through Hopf and pitchfork bifurcations in a parametrically driven nonlinear oscillator, Commun. Nonlinear Sci. Numer. Simul. **37**, 212 (2016).

[7] E. Benoit, J. Callot, F. Diener, and M. Diener, Chasse au canard, Collect. Math. **32**, 37 (1981).

[8] E. Benoit, Linear dynamic bifurcation with noise, in *Dynamic Bifurcations*, edited by E. Benoît (Springer, Berlin, Heidelberg, 1991), pp. 131–150.

[9] P. Szmolyan and M. Wechselberger, Canards in R^3, J. Diff. Equ. **177**, 419 (2001).

[10] P. De Maesschalck, F. Dumortier, and R. Roussarie, *Canard Cycles: From Birth to Transition*, A Series of Modern Surveys in Mathematics, Vol. 73 (Springer International Publishing, Cham, 2021).

[11] P. Ashwin, S. Wieczorek, R. Vitolo, and P. Cox, Tipping points in open systems: Bifurcation, noise-induced and rate-dependent examples in the climate system, Philos. Trans. R. Soc. A **370**, 1166 (2012).

[12] P. Ritchie and J. Sieber, Early-warning indicators for rate-induced tipping, Chaos **26**, 093116 (2016).

[13] P. Ashwin, C. Perryman, and S. Wieczorek, Parameter shifts for nonautonomous systems in low dimension: Bifurcation- and rate-induced tipping, Nonlinearity **30**, 2185 (2017).

[14] C. Kiers, Rate-induced tipping in discrete-time dynamical systems, SIAM J. Appl. Dyn. Syst. **19**, 1200 (2020).

[15] T. Klinker, W. Meyer-Ilse, and W. Lauterborn, Period doubling and chaotic behavior in a driven Toda oscillator, Phys. Lett. A **101**, 371 (1984).

[16] B. Morris and F. Moss, Postponed bifurcations of a quadratic map with a swept parameter, Phys. Lett. A **118**, 117 (1986).

[17] P. Pierański and J. Malecki, Noise-sensitive hysteresis loops around period-doubling bifurcation points, Nuovo Cimento D **9**, 757 (1987).

[18] M. Liauw, K. Koblitz, N. Jaeger, and P. Plath, Periodic perturbation of a drifting heterogeneous catalytic system, J. Phys. Chem. **97**, 11724 (1993).

[19] P. S. Linsay, Period doubling and chaotic behavior in a driven anharmonic oscillator, Phys. Rev. Lett. **47**, 1349 (1981).

[20] R. Kapral and P. Mandel, Bifurcation structure of the nonautonomous quadratic map, Phys. Rev. A **32**, 1076 (1985).

[21] C. Baesens, Slow sweep through a period-doubling cascade: Delayed bifurcations and renormalisation, Physica D **53**, 319 (1991).

[22] C. Baesens, Gevrey series and dynamic bifurcations for analytic slow-fast mappings, Nonlinearity **8**, 179 (1995).

[23] H. Davies and K. Rangavajhula, Dynamic period–doubling bifurcations of a unimodal map, Proc. R. Soc. London, Ser. A **453**, 2043 (1997).

[24] DLMF, NIST digital library of mathematical functions, edited by F. W. J. Olver, A. B. Olde Daalhuis, D. W. Lozier, B. I. Schneider, R. F. Boisvert, C. W. Clark, B. R. Miller, B. V. Saunders, H. S. Cohl, and M. A. McClain, https://dlmf.nist.gov/.